Histol Histopathol (2015) 30: 321-330
DOI: 10.14670/HH-30.321

http://www.hh.um.es

Histology and Histopathology
Cellular and Molecular Biology

Ocular lesions induced in infant rats by busulfan

Tsubasa Saito, Ryo Ando, Toko Ohira, Toru Hoshiya and Kazutoshi Tamura
Pathology Division, Gotemba Laboratories, BoZo Research Center Inc., Kamado, Gotemba, Shizuoka, Japan

Summary. Although busulfan, a bifunctional alkylating agent, is known to induce cataracts in infant rats, the full nature of busulfan-induced ocular lesions has not yet been shown. In order to clarify this point, 6-day-old rats were treated with a single dose of 20 mg/kg busulfan and the ocular tissue was histopathologically and immunohistochemically examined at 1, 2, 4, 7 and 12 days after treatment (DAT). As a result, in the nuclear layer (NL) of the peripheral retina, apoptotic cells significantly increased at 1 DAT and peaked at 2 DAT when cell proliferating activity was depressed. At 4 DAT, the NL showed wavy deformation with formation of rosette-like structures, and these changes progressed prominently at 12 DAT. In addition, a significant reduction in the retinal thickness due to decreased thickness of NL or inner NL was detected at 2 and 4 DAT. On the other hand, in the germinative zone of the lens equator, apoptotic lens epithelial cells significantly increased from 2 to 7 DAT, resulting in partial loss of lens epithelial cells at 7 and 12 DAT. At 12 DAT, prominent swelling and vacuolation of lens fibers were observed in the area from the equatorial zone to the posterior pole, indicating the development of cataract. The present results strongly suggest that prominent apoptosis in component cells was the initial and essential event underlying the development of busulfan-induced ocular lesions in infant rats.

Key words: Busulfan, Infant rat, Ocular lesion, Rosette-like structure, Cataract

Offprint requests to: Tsubasa Saito, BoZo Research Center Inc., 1284, Kamado, Gotemba, Shizuoka 412-0039, Japan. e-mail: tsubasa-saito@outlook.jp

Introduction

Busulfan, a bifunctional alkylating agent, acts on intracellular nucleophiles and proteins and leads to formation of DNA-DNA and DNA-protein cross-links, resulting in DNA damage (Iwamoto et al., 2004; Mertins et al., 2004; Probin et al., 2006; Valdez et al., 2010) and it has been used for treatment of chronic myelogenous leukemia and polycythemia vera and for myeloablative-conditioning regimens before stem cell transplantation.

On the other hand, busulfan has teratogenic potential and induces microtia, micrognathia, microphthalmia and so on (Nagai, 1972; Otsuji et al., 2005; Furukawa et al., 2007; Naruse et al., 2007). In this context, we reported that busulfan induced prominent apoptosis in various tissues including central nervous system (CNS) in rat fetus (Ohira et al., 2009) and that busulfan-induced apoptosis in fetal rat brain was brought about through a p53-mediated pathway (Ohira et al., 2013a). After that, we also reported that busulfan induced apoptosis and inhibition of cell proliferative activity in infant rat cerebellum, which is considered to be continuing to develop after birth (Ohira et al., 2013b). However, the effects of busulfan on the retina, a part of the CNS, have not yet been reported, although it was reported that busulfan induced cataracts in adult humans (Dahlgren et al., 1972; Ravindranathan et al., 1972; Hamming et al., 1976) and infant rats (Solomon et al., 1955; De Beer et al., 1956; Light, 1967).

In the present study, as the first step to clarify the full nature of busulfan-induced ocular toxicity, we examined the nature and sequence of busulfan-induced ocular lesion in infant rats from histopathological and immunohistochemical viewpoints.

Materials and methods

Animals

Male newborn rats were obtained in our laboratory by mating females with males of the same colony of specific pathogen-free rats of the Sprague-Dawley strain purchased from Charles River Japan, Inc. (Kanagawa, Japan). One foster mother with 8 newborns were housed together in plastic Econ cages (W 340 mm x D 450 mm x H 185 mm) with bedding (White flakes: Charles River Japan, Inc.) in an environmentally controlled room (temperature: 23±3°C; relative humidity: 50±20%; ventilation rate: 10-15 times per hour, and 12h/12h light /dark cycle), and fed a commercial diet (NMF; Oriental Yeast Co., Ltd., Tokyo, Japan) and tap water *ad libitum*. A total of 35 6-day-old male rats were subjected to the present experiment. The protocol of this study was reviewed and approved by the Animal Care and Use Committee of BoZo Research Center Inc.

Experimental design

Busulfan (Sigma Aldrich Inc., St. Louis, MO, USA) was suspended with 10 mL/kg of olive oil. Thirty-five male infant rats were divided into the control (n=15) and busulfan (n=20) groups. Our preliminary study indicated that the maximum non-lethal dose of busulfan was 20 mg/kg in infant rats. In the present study, therefore, animals of the busulfan group were treated with 20 mg/kg of busulfan in the dorsal subcutis at 6 days of age. The treated location was under the skin of the back. Animals of the control group received 10 mL/kg of olive oil in the same way. During the experimental period, clinical signs and body weights were checked daily for each animal.

Three animals of the control group and 4 animals of the busulfan group were killed under isoflurane anesthesia at 1, 2, 4, 7 and 12 days after treatment (DAT), respectively, and they were subjected to histopathological and immunohistochemical examinations.

Histopathology

The eyeballs were fixed with Davidson's solution at 4°C, and preserved in 10% neutral buffered formalin until histopathological examination. Paraffin sections were stained with hematoxylin and eosin (HE). Fig. 1 shows the HE-stained sagittal section of the eye used for histopathological examination in the present study.

Additional sections from each animal were subjected to *in situ* detection of fragmented DNA by the terminal deoxynucleotidyl transferase-mediated dUTP nick-end labeling (TUNEL) method using an apoptosis detection kit (ApopTag Peroxidase In Situ Apoptosis Detection Kit, Chemicon Inc., Gaithersburg, MD, USA) according to the manufacturer's instructions. In brief, multiple fragmented DNA 3'-OH ends on the section were labeled with digoxigenin-dUTP in the presence of terminal deoxynucleotidyl transferase. Peroxidase-conjugeted anti-digoxigenin antibody was then added to the sections. Apoptotic nuclei were visualized by DAB reaction. The sections were then counterstained with methyl green.

Immunohistochemistry

The primary antibodies used were as follows: rabbit anti-cleaved caspase-3 polyclonal antibody (1:200, Cell Signaling Technology, Beverly, MA, USA) as a marker for apoptotic cells, rabbit anti-phospho-histone H3 polyclonal antibody (1:150, Cell Signaling Technology) as a marker for M phase cells, and rabbit anti-proliferating cell nuclear antigen (PCNA) monoclonal antibody (1:200, Dako Japan) as a marker for G1 to S phase cells. Immunohistochemical staining was done

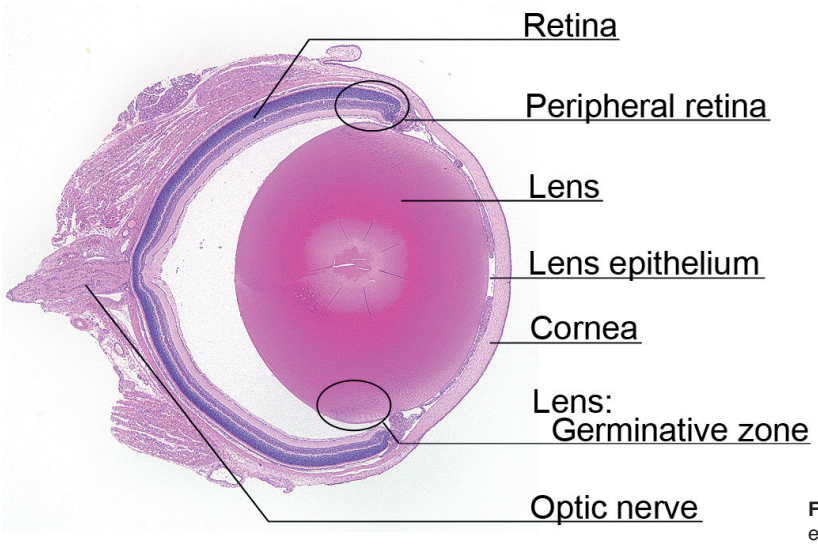

Fig. 1. Sagittal section of the eye used for histopathological examination. HE stain.

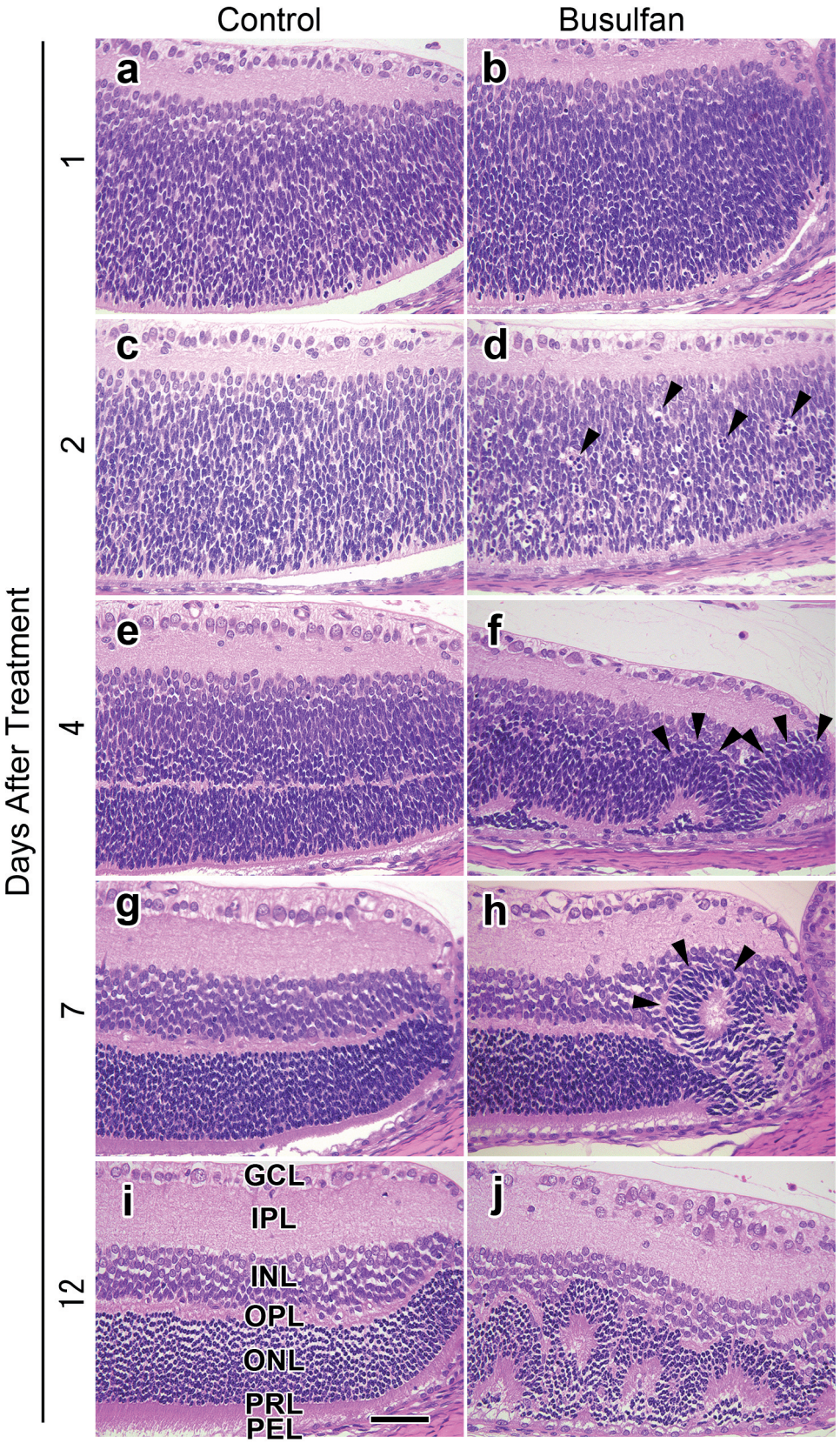

Fig. 2. Sequential histopathological findings in the peripheral retina of the control **(a, c, e, g and i)** and busulfan groups **(b, d, f, h and j)** at 1 **(a, b)**, 2 **(c, d)**, 4 **(e, f)**, 7 **(g, h)** and 12 DAT **(i, j)**. Arrowheads: pyknosis **(d)**, wavy deformation with formation of rosette-like structure **(f)**, rosette-like structures **(h)** marked wavy deformation with the prominent formation of rosette-like structures **(j)**. GCL: ganglion cell layer; IPL: inner plexiform layer; INL: inner nuclear layer; OPL, outer plexiform layer: ONL, outer nuclear layer, PRL: photoreceptor layer; and PEL: pigment epithelial layer. HE Stain. Bar: 50 µm.

using Dako EnVision kits/HRP (DAB) (Dako Japan, Kyoto). Antigen retrieval for some antibodies was performed by heating the sections in the autoclave (121°C for 20 min; anti-cleaved caspase-3) or microwave oven (95°C for 15 min; phospho-histone H3 and PCNA), and then the sections were incubated in 10 mM citrate buffer, pH 6.0, and 0.1% trypsin (37°C for 15 min; PCNA). Endogenous peroxidase activity was quenched by immersing the sections in 3% H_2O_2 in methanol for 10 min, and each section was left at 4°C overnight, and then reacted with Envision$^+$ kit (Dako Japan, Kyoto, Japan) at room temperature for 30 min. Positive signals were visualized by peroxidase-diaminobenzidine reaction and then counterstained with hematoxylin.

Morphometric analysis

To evaluate apoptosis and mitotic activities in the retina and lens epithelium, the labeling indices (%) of TUNEL- and phospho-histone H3-positive cells were calculated by counting 500 cells in the peripheral region of the retina and by counting all cells in the germinative zone of the lens under a microscope at a magnification of 200. Measurements of the retinal thickness in the peripheral and central retina were performed using a digital camera (FX380; Olympus, Tokyo, Japan) with an image filing software (FLVFS-LS; Flovel, Tokyo, Japan). In the busulfan group, measurement of the peripheral retina was measured in an area adjacent to wavy and rosette-like structure to avoid these deformation regions. Each labeling index (%) and retinal thickness (μm) was represented as the mean ± standard deviation (SD).

Statistical analysis

All data were expressed as the mean ± SD. We adopted the Student's t-test or the Welch's t-test according to the result of the *F*-test. P-values less than 5% ($p<0.05$) and 1% ($p<0.01$) were considered as a statistically significant.

Results

Clinical findings

There were no significant differences in the bodyweight gain between the two groups, although the bodyweight gain was slightly depressed in the busulfan group. Throughout the experimental period, only one animal in the busulfan group died at 12 DAT.

Histopathological and immunohistochemical findings

Retina

At 1 and 2 DAT (i.e. 7 and 8 days of age), the

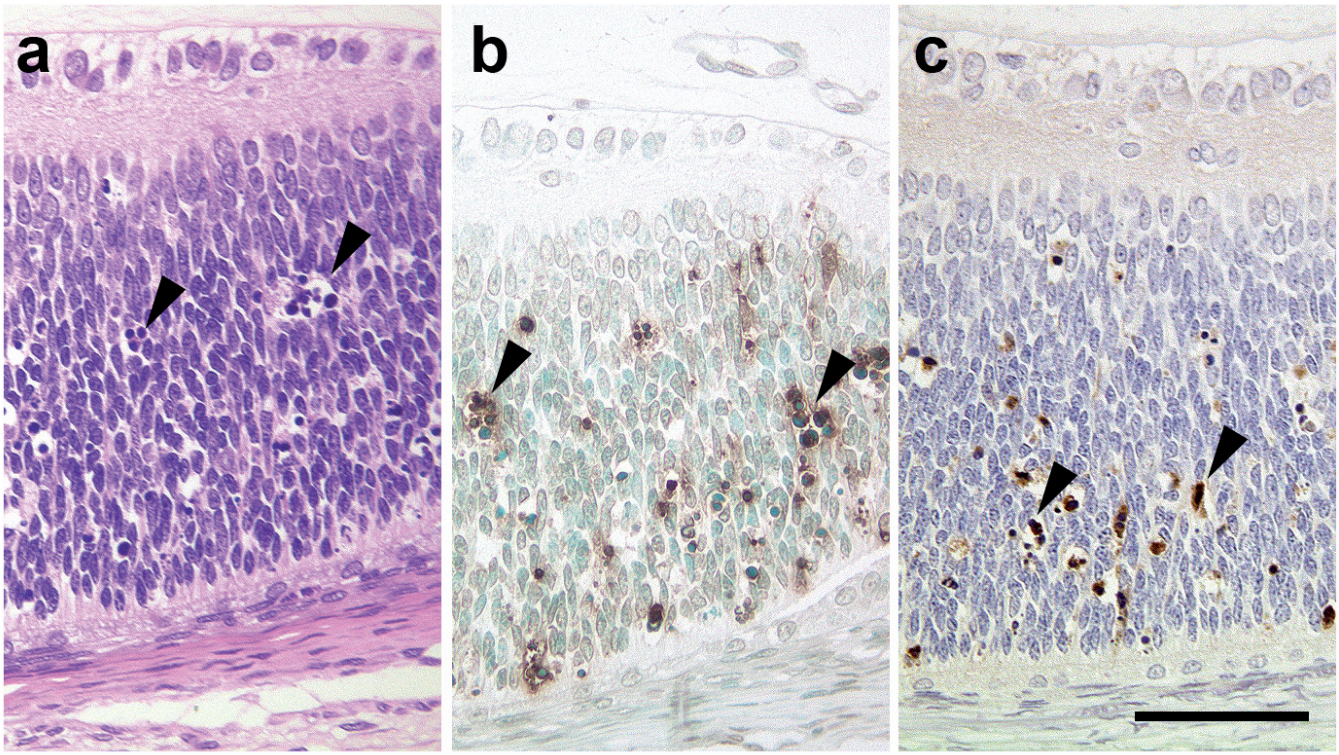

Fig. 3. The peripheral retina of the busulfan group at 2 DAT. Pyknotic cells (**a**, arrowheads) are TUNEL - (**b**, arrowheads) and cleaved caspase-3 - positive (**c**, arrowheads). a: HE stain, b: TUNEL method, and c: immunostaining. Bar: 50 µm.

peripheral retina mainly consisted of the ganglion cell layer (GCL), inner plexiform layer (IPL), and wide single nuclear layer (NL) composed of tightly packed undifferentiated neuroblastic cells (Fig. 2a-d). In the control group, a small number of mitotic cells and a few pyknotic ones were observed in the basal layer of the NL at 1 and 2 DAT (Fig. 2a,c). On the other hand, in the busulfan group, histopathological changes were mainly observed in the peripheral region of the retina, where a small number of mitotic cells as well as pyknotic ones were observed in the basal layer of NL at 1 DAT (Fig. 2b) and many pyknotic cells throughout the NL at 2 DAT (Fig. 2d).

At 4 DAT (i.e. 10 days of age), the NL in the control group was separated into the inner (INL) and outer NL (ONL) by the outer plexiform layer (OPL) between them (Fig. 2e). On the other hand, separation of the INL from the ONL was not distinct in the busulfan group (Fig. 2f). However, the INL was somewhat thinner than that in the control group (Fig. 2e,f) and the NL showed wavy deformation with formation of rosette-like structures.

At 7 DAT (i.e. 13 days of age), the construction of retinal layers was almost established (Fig. 2g,h). In the busulfan group, formation of rosette-like structures was observed in the ONL (Fig. 2h).

At 12 DAT (i.e. 19 days of age), as compared with the control group (Fig. 2i), the retinal construction was disordered in the busulfan group (Fig. 2j). Namely, the whole ONL showed marked wavy deformation with the prominent formation of rosette-like structures (Fig. 2j). In addition, although the PEL remained intact and detachment of the retina from the PEL was not detected, the OPL and PRL became indistinct (Fig. 2j). The above-

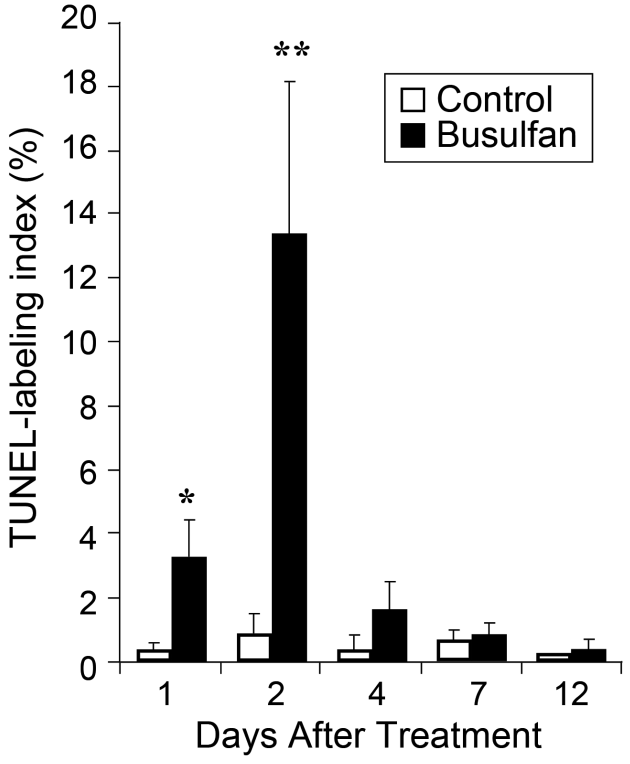

Fig. 4. Changes in the TUNEL-labeling index in the peripheral retina. Each value represents mean ± SD. *p<0.05 and **p<0.01: Significantly different from the control group.

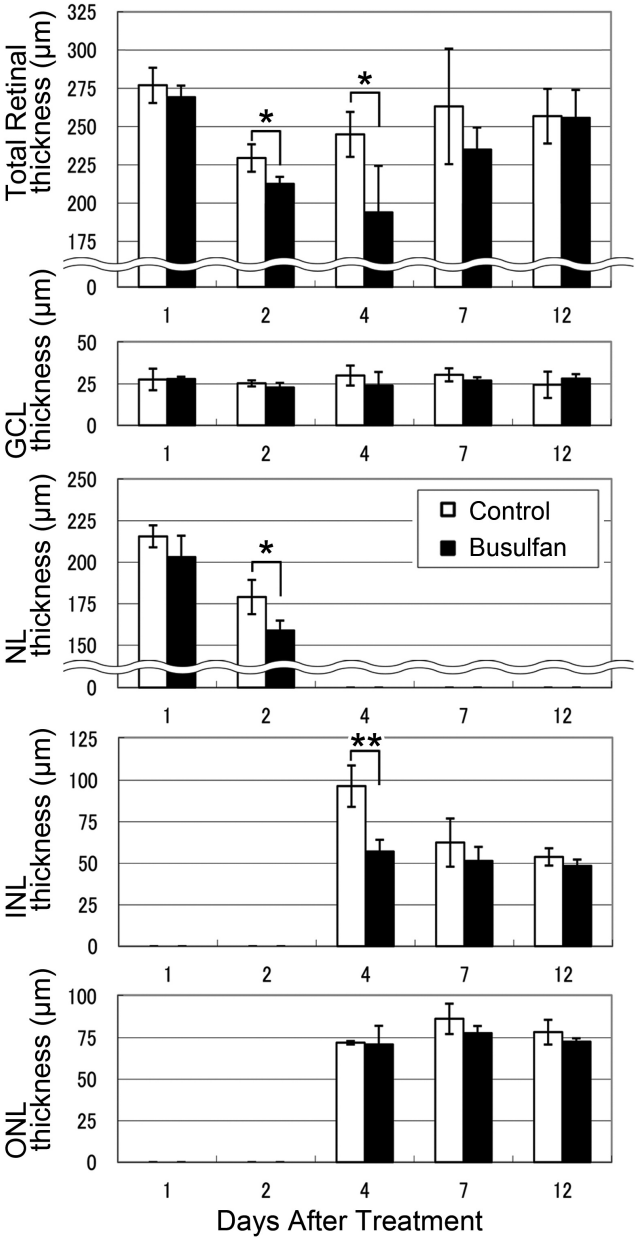

Fig. 5. Changes in the thicknesses of the whole retina and each layer in the peripheral retina. The NL are separated into the INL and ONL at and after 4 DAT. Each value represents mean ± SD. *p<0.05 and **p<0.01: Significantly different from the control group.

mentioned changes in the peripheral retina were not detected in the central retina throughout the experimental period.

Most of the above-mentioned pyknotic nuclei (Fig. 3a) seen in the NL were TUNEL- (Fig. 3b) and cleaved caspase-3-positive (Fig. 3c), indicating that the pyknotic cells were apoptotic. In the busulfan group, the TUNEL-labeling index significantly increased at 1 DAT, peaked at 2 DAT, and returned close to the control level at 4 DAT (Fig. 4). The peripheral retinal thickness was significantly reduced at 2 and 4 DAT due to the decreased thickness of NL at 2 DAT and that of INL at 4 DAT (Fig. 5).

In the NL at 2 DAT, many PCNA-positive cells were detected especially in the upper layer in the control group (Fig. 6a). In the busulfan group, the number of PCNA-positive cells was smaller in the busulfan group than in the control group (Fig. 6b). At 4 DAT, PCNA-positive cells were detected in the INL, showing a prominent decrease in number in both groups (Fig. 6c,d). In addition, a few PCNA-positive cells were also detected in the ONL in the busulfan group (Fig. 6d). At the bottom of NL, a few phospho-histone H3-positive cells were detected in both the control (Fig. 7a) and busulfan groups (Fig. 7b) from 1 to 4 DAT, and the phospho-histone H3-labeling index showed no

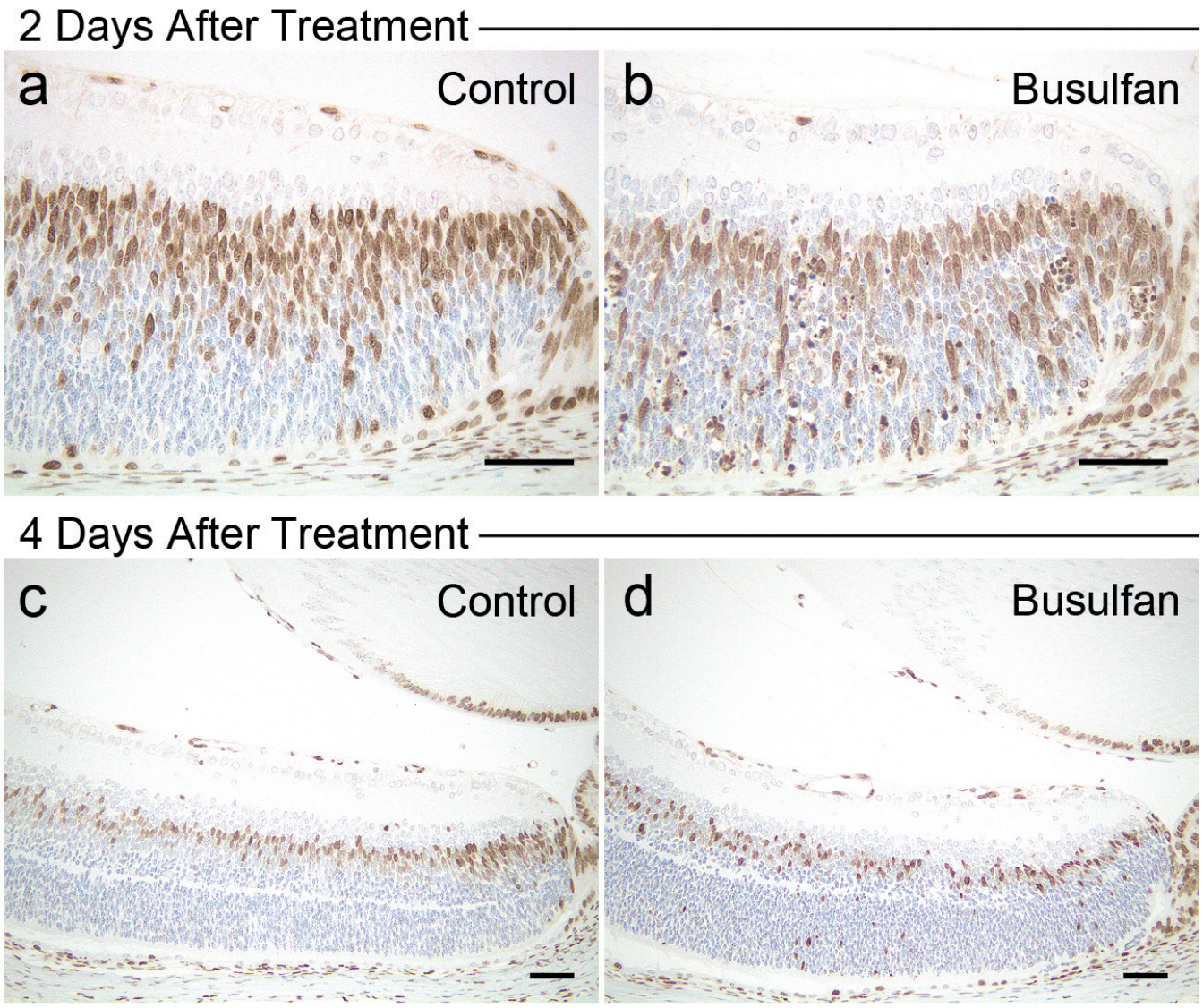

Fig. 6. Distribution of PCNA-positive cells in the peripheral retina of the control **(a, c)** and busulfan groups **(b, d)** at 2 **(a, b)** and 4 DAT **(c, d)**. As compared with the control group **(a)**, At 2 DAT, the number of PCNA-positive cells is prominently reduced in the busulfan group **(b)**. Immunostaining, Bars: a, b, 50 μm; c, d, 100 μm.

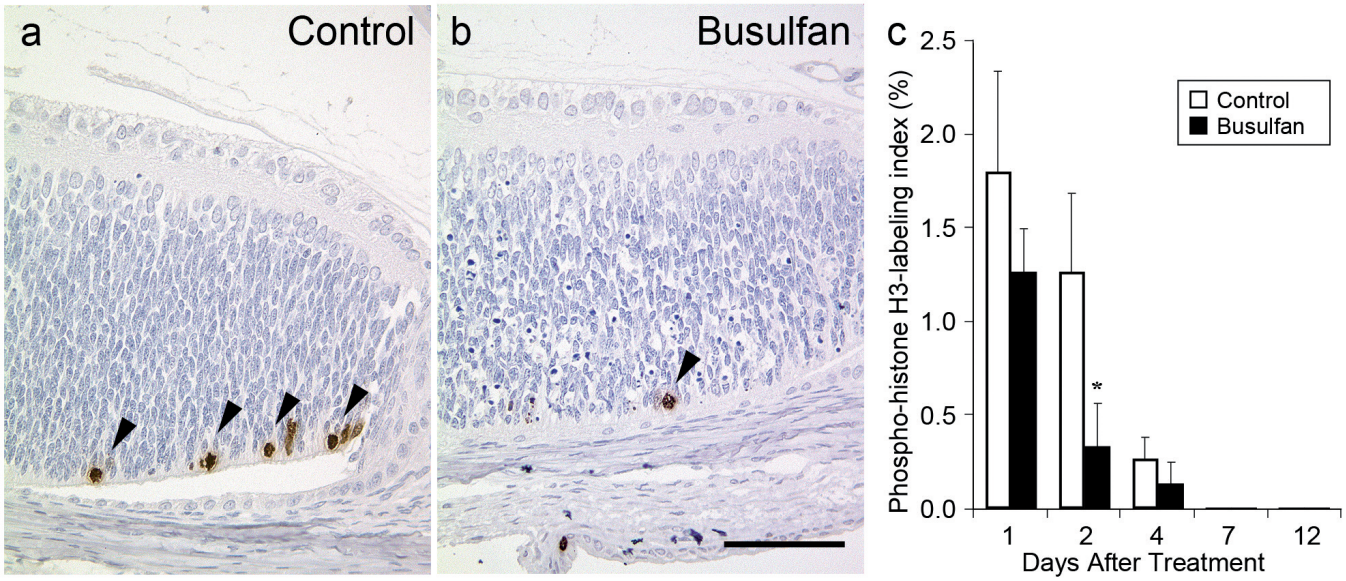

Fig. 7. Distribution of phospho-histone H3-positive cells (arrowheads) in the retina of the control **(a)** and busulfan groups **(b)** at 2 DAT. Immunostaining, Changes in the phospho-histone H3-labeling index in the peripheral retina **(c)**. The value represents mean ± SD. *p<0.05: Significantly different from the control group. Bar: 50 μm.

significant differences between the two groups except for that at 2 DAT (Fig. 7c).

Lens

There were no pyknotic lens epithelial cells observed in the control group. On the other hand, in the lens epithelium in the busulfan group, the TUNEL-labeling index significantly increased from 2 to 7 DAT, showing the peak level at 4 DAT, in the germinative zone of the lens equator (Fig. 8). Most of the pyknotic nuclei of lens epithelial cells were TUNEL- and cleaved caspase-3-positive (Fig. 9a-c), indicating that the pyknotic cells were apoptotic. On the other hand, the phospho-histone H3-labeling index showed no significant differences between the two groups (data not shown).

As compared with the control group (Fig. 9d), lens epithelial cells in the busulfan group partially disappeared at 7 and 12 DAT (Fig. 9e). In addition, prominent swelling and vacuolation of lens fibers developed in the posterior region of the lens at 12 DAT (Fig. 9f,g), indicating the development of cataract.

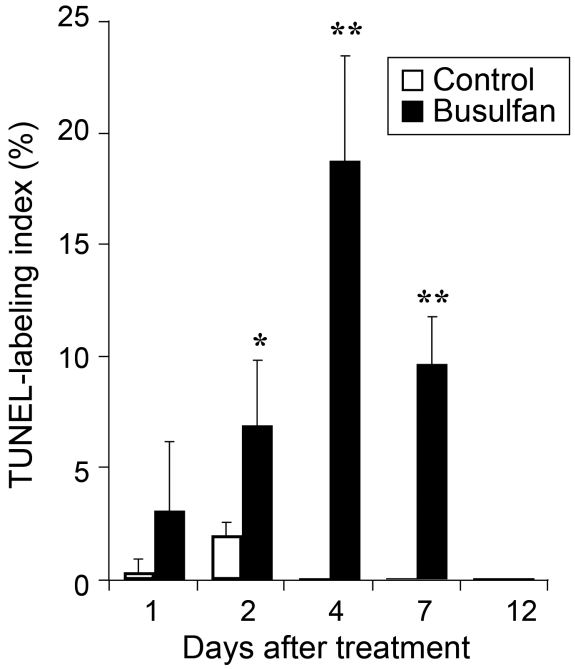

Fig. 8. Changes in the TUNEL-labeling index in the lens epitheliun in the germinative zone. Each value represents mean ± SD. *p<0.05 and **p<0.01: Significantly different from the control group.

Discussion

In the present study, the nature and sequence of ocular lesions induced in infant rats exposed to busulfan (20 mg/kg b.w.) at 6 days of age were examined up to 12 DAT.

In the retina, busulfan-related histopathological changes were mainly observed in the peripheral region where many proliferating cells usually exist. Namely, apoptotic cells significantly increased at 1 DAT and peaked at 2 DAT when cell proliferative activity evaluated by the number of PCNA-positive cells was depressed compared with the control group. Thus, in

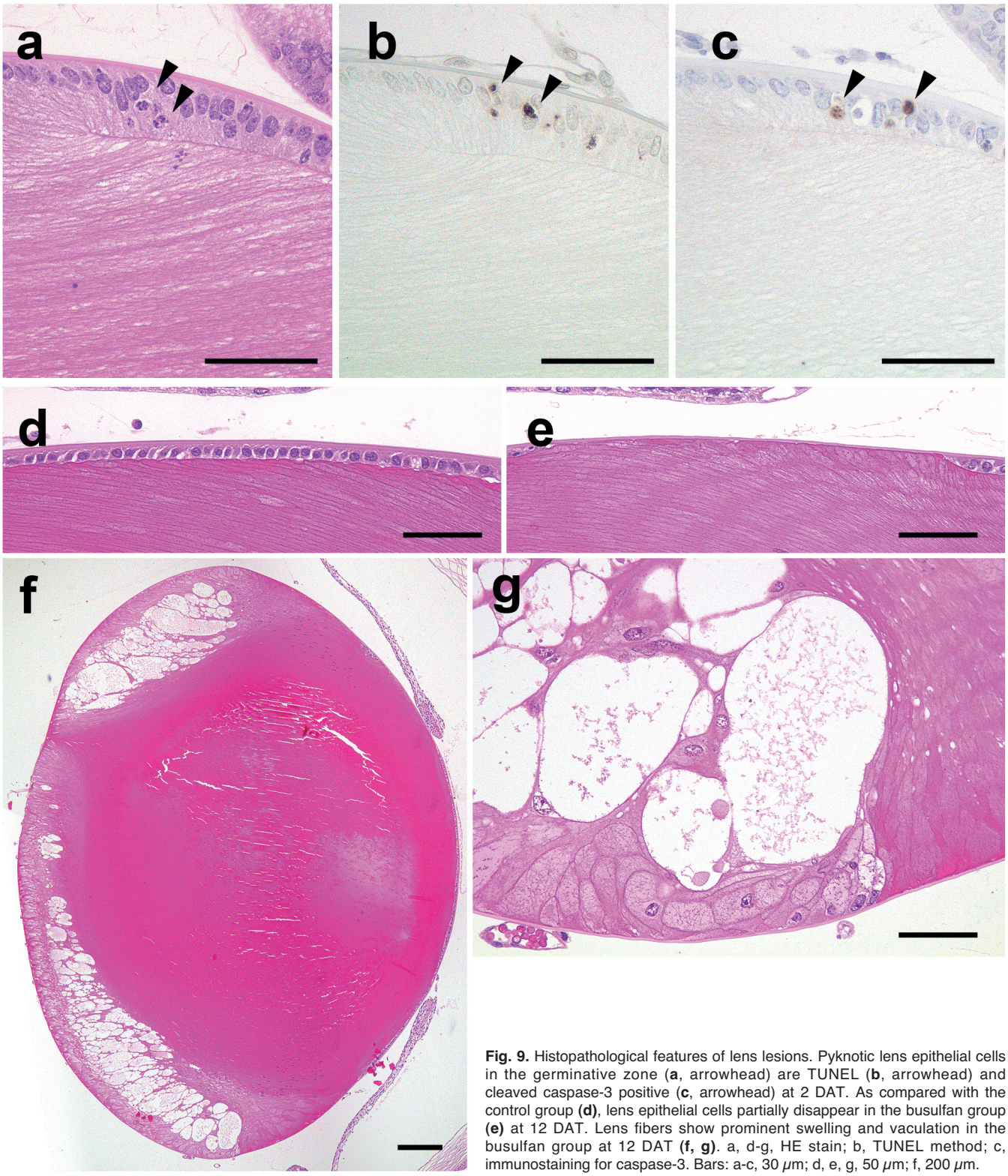

Fig. 9. Histopathological features of lens lesions. Pyknotic lens epithelial cells in the germinative zone (**a**, arrowhead) are TUNEL (**b**, arrowhead) and cleaved caspase-3 positive (**c**, arrowhead) at 2 DAT. As compared with the control group (**d**), lens epithelial cells partially disappear in the busulfan group **(e)** at 12 DAT. Lens fibers show prominent swelling and vaculation in the busulfan group at 12 DAT **(f, g)**. a, d-g, HE stain; b, TUNEL method; c, immunostaining for caspase-3. Bars: a-c, 30 μm; d, e, g, 50 μm; f, 200 μm.

infant rats, busulfan induced apoptosis and depression of cell proliferative activity in the retina as previously reported in the cerebellum (Ohira et al., 2013b).

At 4 DAT, the NL was divided into two distinct layers, i.e. INL and ONL, in the control group. On the other hand, separation of ONL from INL was delayed and the NL showed wavy deformation with formation of rosette-like structures in the busulfan group. Such a delay in the establishment of the two distinct layers in the busulfan group is considered to be brought about by prominent loss of component cells through apoptosis, together with depression of cell proliferative activity in the NL at 2 DAT. At 12 DAT, the retinal construction was completed in the control group while it was disordered in the busulfan group. The whole ONL showed marked wavy deformation with prominent formation of rosette-like structures.

Retinal lesions of a similar nature were also previously reported after treatment with various DNA-damaging agents such as cytosine arabinoside (Percy and Danylchuk, 1977), paclitaxel (Kuwata et al., 2009), sisplatine (Yang et al., 2000) and N-methyl-N-nitrosourea (MNU) (Nambu et al., 1998) and after radiation therapy (Glücksmann and Tansley, 1936; Shively et al., 1970). In those cases, the retinal changes were suggested to be brought about by loss of normal contact between retinal cells and the pigment epithelium (Polyak et al., 1996), selective cell death in the neuroblastic layer (Kuwata et al., 2009) and/or incomplete repair due to imbalance of abnormal cell death and cell proliferation caused (Nambu et al., 1998). The retinal changes observed in the present study may also be induced through similar mechanisms. In particular, tissue destruction by enhanced apoptotic cell death with incomplete repair and subsequent breaking down of intact retinal cell connection seemed to be involved in the formation of rossete-like structures by retinal cells in the ONL. In this context, the formation of rosette-like strictures by neuroepithelial cells was reported in the ventricular zone of telencephalic wall of fetal rat brain after treatment with 5-azacytidine (Ueno et al., 2002) or ethylnitrosourea (Fujiwara, 1980). In those cases, the pathogenesis of formation of rosette-like structures was suggested as follows. Tissue destruction by enhanced apoptosis might break the connections of neuroepithelial cells and lead intact neuroepithelial cells to form new structures such as rosette-like tubules (Ueno et al., 2002).

In the lens, apoptosis of lens epithelial cells appeared as the earliest change in the germinative zone of the lens quarter, the site of cell proliferation. It increased significantly from 2 to 7 DAT, showing the peak level at 4 DAT. Subsequently, lens epithelial cells partially disappeared at 7 and 12 DAT, followed by swelling and vacuolation of lens fibers in the posterior region of the lens. Such degenerative changes of lens fibers indicated the development of cataracts, and lens epithelial cell apoptosis was suggested to be an early and common event in the development of busulfan-induced cataract as previously reported in non-congenital cataract (Li et al., 1995) and UVB-induce cataract (Li and Spector, 1996).

In addition to busulfan (Solomon et al., 1955; De Beer et al., 1956; Light, 1967), MNU (Yoshizawa et al., 2000; Kiuchi et al., 2002; Miki et al., 2007) and paclitaxel (Kuwata et al., 2009) were also reported to induce cataracts in rodent neonates or infants. In addition, our preliminary study showed that busulfan did not induce cataracts in adult rats (data not shown). Moreover, it is known that mitotic activity of lens epithelial cells is higher in infant rats than in adult rats (Mikulicich and Young, 1963) and that the main target of cytotoxic effects of busulfan is proliferating cells. Therefore, the age-dependent difference in the induction of cataracts may be due to the difference in the susceptibility of lens epithelial cells to busulfan. It is also suggested that the age-related difference in the induction of cataract may be due to the difference in the drug delivery system between neonates and adults. In adult humans cataracts developed as side-effects of busulfan therapy usually after prolonged administration (Honda et al., 1993; Soysal et al., 1993) or short-term administration of large doses (Kaida et al., 1999).

Finally, although it was said that busulfan induced cell cycle arrest in various types of cells (Millar et al., 1986; Ritter et al., 2002; Valdez et al., 2010), cell cycle analysis in the ocular tissue after busulfan treatment was left as our future primary consideration.

In conclusion, the present study on the nature and sequence of busulfan-induced ocular lesions in infant rats strongly suggested that prominent apoptosis in the retina and lens epithelium was the initial and essential event underlying the development of ocular lesions. The present results will provide fundamental and useful information on chemical-induced ocular lesions.

Acknowledgements. The authors gratefully acknowledge Dr. Kunio Doi, Professor Emeritus of the University of Tokyo, for critical review of the manuscript, and Mr. Pete Aughton, ITR Laboratories Canada Inc., for language editing of this paper.

References

De Beer E.J., Light A.E. and Solomon C. (1956). Effects of dietary supplements in preventing or augmenting the production of cataracts in rats by 1, 4-dimethanesulfonoxybutane. J. Nutr. 10, 157-172.

Dahlgren S., Holm G., Svanborg N. and Watz R. (1972). Clinical and morphological side-effects of busulfan (Myleran) treatment. Acta Med. Scand. 192, 129.135.

Fujiwara H. (1980). Cytotoxic effects of ethylnitrosourea on central nervous system of rat embryo. Special references to carcinogenesis and teratogenesis. Acta Patol. Jpn. 30, 375-387.

Furukawa S., Usuda K., Abe M. and Ogawa I. (2007). Microencephaly and microphthalmia in rat fetuses by busulfan. Histol. Histopathol. 22, 389-397.

Glücksmann A. and Tansley K. (1936). Some effects of gamma

radiation on the developing rat retina. Br. J. Ophthalmol. 20, 497-509.

Hamming N.A., Apple D.J. and Goldberg M.F. (1976). Histopathology and ultrastructure of busulfan-induced cataract. Albrecht Von Graefes Arch. Klin. Exp. Ophthalmol. 200. 139-147.

Honda A., Dake Y. and Amemiya T. (1993). Cataracts in a patient treated with busulfan (Mablin powder) for eight years. Nihon Ganka Gakkai Zasshi. 97, 1242-1245.

Iwamoto T., Hiraku Y., Oikawa S., Mizutani H., Kojima M. and Kawanishi S. (2004). DNA intrastrand cross-link at the 5'-GA-3' sequence formed by busulfan and its role in the cytotoxic effect. Cancer Sci. 95, 454-458.

Kaida T., Ogawa T. and Amemiya T. (1999). Cataract induced by short-term administration of large doses of busulfan: a case report. Ophthalmologica 213, 397-399.

Kiuchi K., Yoshizawza K., Moriguchi K. and Tsubura A. (2002). Rapid induction of cataract by a single intraperitoneal administration of N-methyl-N-nitrosourea in 15-day-old Sprague-Dawley (Jcl: SD) rats. Exp. Toxicol. Pathol. 54, 181-186.

Kuwata M., Yoshizawa K., Matsumura M., Takahashi K. and Tsubura A. (2009). Ocular toxicity caused by Paclitaxel in neonatal sprague-dawley rats. In Vivo 23, 555-560.

Li W.C. and Spector A. (1996). Lens epithelial cell apoptosis is an early event in the development of UVB-induced cataract. Free Radic. Biol. Med. 20, 301-311.

Li W.C., Kuszak J.R., Dunn K., Wang R.R., Ma W., Wang G.M., Spector A., Leib M., Cotliar A.M. and Weiss M. (1995). Lens epithelial cell apoptosis appears to be a common cellular basis for non-congenital cataract development in humans and animals. J. Cell Biol. 1995 130, 169-181.

Light A.E. (1967). Additional observations on the effects of busulfan on cataract formation, duration of anesthesia, and reproduction in rats. Toxicol. Appl. Pharmacol. 10, 459-466.

Mertins S.D., Myers T.G., Holbeck S.L., Medina-Perez W., Wang E., Kohlhagen G., Pommier Y. and Bates S.E. (2004). In vitro evaluation of dimethane sulfonate analogues with potential alkylating activity and selective renal cell carcinoma cytotoxicity. Mol. Cancer Ther. 3, 849-860.

Miki K., Yoshizawa K., Uehara N., Yuri T., Matsuoka Y. and Tsubura A. (2007). PARP inhibitors accelerate N-methyl-N-nitrosourea-induced cataractogenesis in Sprague-Dawley rats. In Vivo 21, 739-744.

Mikulicich A.G. and Young R.W. (1963). Cell proliferation and displacement in the lens epithelium of young rats injected with tritiated thymidine. Invest. Ophthalmol. 2, 344-354.

Millar B.C., Tilby M.J., Ormerod M.G., Payne A.W., Jinks S. and Loverock P.S. (1986). Comparative studies of total cross-linking, cell survival and cell cycle perturbations in Chinese hamster cells treated with alkylating agents in vitro. Biochem. Pharmacol. 35, 1163-1169.

Nagai H. (1972). Effects of transplacentally injected alkylating agents upon development of embryos. Appearance of intrauterine death and mesodermal malformation. Bull. Tokyo Dent. Coll. 13, 103-119.

Nambu H., Yoshizawa K., Yang J., Yamamoto D. and Tsubura A. (1998). Age-specific and dose-dependent retinal dysplasia and degeneration induced by a single intraperitoneal administration of N-Methyl-N-nitrosourea to rats. J. Toxicol. Pathol. 11, 127-131.

Naruse T., Takahara M., Takagi M., Oberg K.C. and Ogino T. (2007). Busulfan-induced central polydactyly, syndactyly and cleft hand or foot: a common mechanism of disruption leads to divergent phenotypes. Dev. Growth Differ. 49, 533-541.

Ohira T., Ando R., Andoh R., Nakazawa T., Nishihara K., Yamamoto S., Nakamura N. and Tamura K. (2009). Distribution and sequence of pyknotic cells in rat fetuses exposed to busulfan. J. Toxicol. Pathol. 22, 167-171.

Ohira T., Ando R., Okada Y., Suzuki H., Saito T., Nakazawa T., Nishihara K., Yamamoto S., Nakamura N. and Tamura K. (2013a). Sequence of busulfan-induced neural progenitor cell damage in the fetal rat brain. Exp. Toxicol. Pathol. 65, 523-530.

Ohira T., Ando R., Saito T., Yahata M., Oshima Y. and Tamura K. (2013b). Busulfan-induced pathological changes of the cerebellar development in infant rats. Exp. Toxicol. Pathol. 65, 789-797.

Otsuji M., Takahara M., Naruse T., Guan D., Harada M., Zhe P., Takagi M. and Ogino T. (2005). Developmental abnormalities in rat embryos leading to tibial ray deficiencies induced by busulfan. Birth Defects Res. A Clin. Mol. Teratol. 73, 461-467.

Percy D.H. and Danylchuk K.D. (1977). Experimental retinal dysplasia due to cytosine arabinoside. Invest. Ophthalmol. Vis. Sci. 16, 353-364.

Polyak K., Waldman T., He T.C., Kinzler K.W. and Vogelstein B. (1996). Genetic determinants of p53-induced apoptosis and growth arrest. Genes Dev. 10, 1945-1952.

Probin V., Wang Y., Bai A. and Zhou D. (2006). Busulfan selectively induces cellular senescence but not apoptosis in WI38 fibroblasts via a p53-independent but extracellular signal-regulated kinase-p38 mitogen-activated protein kinase-dependent mechanism. J. Pharmacol. Exp. Ther. 319, 551-560.

Ravindranathan M.P., Paul V.J. and Kuriakose E.T. (1972). Cataract after busulphan treatment. Br. Med. J. 1, 218-219.

Ritter C., Sperker B., Grube M., Dressel D., Kunert-Keil C. and Kroemer H.K. (2002). Overexpression of glutathione S-transferase A1-1 in ECV 304 cells protects against busulfan mediated G2-arrest and induces tissue factor expression. Br. J. Pharmacol. 137, 1100-1106.

Shively J.N., Phemister R.D., Epling G.P. and Jensen R. (1970). Pathogenesis of radiation-induced retinal dysplasia. Invest. Ophthalmol. 9, 888–900.

Solomon C., Light A.E. and De Beer E.J. (1955). Cataracts produced in rats by 1, 4-dimethanesulfonoxybutane (myleran). AMA Arch. Ophthalmol. 54, 850-852.

Soysal T., Bavunoğlu I., Başlar Z. and Aktuğlu G. (1993). Cataract after prolonged busulphan therapy. Acta Haematol. 90, 213.

Ueno M., Katayama K., Yasoshima A., nakayama H. and Doi K. (2002). 5-Azacytidine-induced histopathological changes in the central nervous system of rat fetuses. Exp. Toxic Pathol. 54, 91-96.

Valdez B.C., Li Y., Murray D., Corn P., Champlin R.E. and Andersson B.S. (2010). 5-Aza-2'-deoxycytidine sensitizes busulfan-resistant myeloid leukemia cells by regulating expression of genes involved in cell cycle checkpoint and apoptosis. Leuk. Res. 34, 364-372.

Yang J., Yoshizawa K., Shikata N., Kiyozuka Y., Senzaki H. and Tsubura A. (2000). Retinal damage induced by cisplatin in neonatal rats and mice. Curr. Eye Res. 20, 441-446.

Yoshizawa K., Oishi Y., Nambu H., Yamamoto D., Yang J., Senzaki H., Miki H. and Tsubura A. (2000). Cataractogenesis in Neonatal Sprague-Dawley Rats by N-Methyl-N-Nitrosourea. Toxicol. Pathol. 28, 555-564.

Accepted September 26, 2014